DOI: 10.1002/cmdc.200600243

Molecular Dynamics Simulations of Na^+/Cl^--Dependent Neurotransmitter Transporters in a Membrane-Aqueous System

Anne Marie Jørgensen,[a, b] Lena Tagmose,[b] Anne Marie M. Jørgensen,[b] Klaus P. Bøgesø,[c] and Günther H. Peters*[a]

We have performed molecular dynamics simulations of a homology model of the human serotonin transporter (hSERT) in a membrane environment and in complex with either the natural substrate 5-HT or the selective serotonin reuptake inhibitor escitalopram. We have also included a transporter homologue, the Aquifex aeolicus leucine transporter (LeuT), in our study to evaluate the applicability of a simple and computationally attractive membrane system. Fluctuations in LeuT extracted from simulations are in good agreement with crystallographic B factors. Furthermore, key interactions identified in the X-ray structure of LeuT are maintained throughout the simulations indicating that our simple membrane system is suitable for studying the transmembrane protein hSERT in complex with 5-HT or escitalopram. For these transporter complexes, only relatively small fluctuations are observed in the ligand-binding cleft. Specific interactions responsible for ligand recognition, are identified in the hSERT–5HT and hSERT–escitalopram complexes. Our findings are in good agreement with predictions from mutagenesis studies.

Introduction

Monoamine transporters are members of the neurotransmitter:sodium symporter (NSS) family, which is characterized by a 12 α-helical domain (12 transmembrane (TM)) that spans the plasma membrane. Three transporters within this family, the dopamine, the norepinephrine, and the serotonin transporter (DAT, NET, and hSERT, respectively), are responsible for taking up their respective neurotransmitter from the synaptic cleft after release during neurotransmission.[1,2] Each of these are important targets for drugs of abuse such as cocaine and amphetamines.[3–5] The serotonin transporter (hSERT), in particular, is the site of action for antidepressants, such as imipramine and the selective serotonin reuptake inhibitors (SSRI), paroxetine, fluoxetine, and sertraline, and for the combined SSRI/allosteric serotonin reuptake inhibitor (ASRI) escitalopram.[6,7] As the major target for treatment of mood disorders, including major depression, anxiety, post-traumatic stress, and obsessive-compulsive disorders, structural aspects of hSERT—and how these relate to its function and antagonist recognition—are of major interest in the pharmaceutical industry. At the present time, no X-ray structure is available for this target, but pharmacophore and homology modeling approaches have been used to gain insights into essential protein–ligand interaction patterns in three dimensions.[8–14] Various homology models have previously been constructed for the monoamine transporters. However, these have been based on the X-ray structures of 12TM transporters from the major facilitator superfamily (MFS) and from the NhaA antiporter family.[10–14] Even though 12TM α-helical domains dominate the secondary structure of MFS and NhaA members, their tertiary structures differ significantly from that of NSS proteins.[15–20]

An X-ray structure of a bacterial NSS, the *Aquifex aeolicus* leucine transporter (LeuT) has recently become available and provides insight into the 12TM motif for this group of transporters.[18] The 12TM motif found in LeuT is believed to be an appropriate model for other NSSs, including the human serotonin transporter (hSERT).[21,22] LeuT has already been used as a template for modeling hSERT. However, the described models do not provide insight into protein–ligand interactions.[23–25] One of the major challenges in the optimization/refinement of a homology model is to include the biological matrix in which proteins function. It is well-known that the environment represents one of the crucial factors which determine the native protein conformation.[26,27] Changes in the properties of the environment may induce conformational changes of both globular[28] and membrane proteins, thereby affecting protein–ligand contacts and specific protein–protein and protein–water interactions. Properties of all three kinds are likely to be affected when going from one transporter to another or when a pro-

[a] *A. M. Jørgensen, Assoc. Prof. G. H. Peters*
MEMPHYS-Center for Biomembrane Physics, Department of Chemistry, Technical University of Denmark, Building 206, 2800 Kgs. Lyngby (Denmark)
Fax: (+45) 45-88-31-36
E-mail: ghp@kemi.dtu.dk

[b] *A. M. Jørgensen, Dr. L. Tagmose, Dr. A. M. M. Jørgensen*
Department of Computational Chemistry, H. Lundbeck A/S, 9 Ottiliavej, 2500 Valby (Denmark)

[c] *Dr. K. P. Bøgesø*
Lundbeck Research Denmark, H. Lundbeck A/S, 9 Ottiliavej, 2500 Valby (Denmark)

Supporting information for this article is available on the WWW under http://www.chemmedchem.org or from the author.

tein model that has been constructed in vacuo is inserted into a membrane system.[26,29] To overcome this shortcoming, different refinement methods have been developed, spanning from static to dynamic approaches. In the former approaches, the varying properties of the protein environment are taken into consideration by applying different physicochemical constraints to protein residues, depending on their spatial location.[30] Such methods have for instance been employed for the construction of G-protein-coupled-receptor (GPCR) three-dimensional models.[31] In the dynamic approaches, protein models are refined by various kinds of simulation approaches. Prior to the simulation, the models are usually embedded in an environment sharing physicochemical properties with a lipid bilayer.[32] Such an approach has for instance been applied for the optimization of GPCR receptor homology models in membranes or simplified membrane systems.[33–37] The literature provides numerous examples of molecular dynamics (MD) simulation studies of membrane proteins in explicit lipid bilayers,[38–44] simplified membrane–water systems, such as the octane slab developed by Sansom's lab,[43,45] and uniform solvent dielectric models.[46] Performing MD simulations of membrane proteins in explicit bilayer systems is an often applied approach to study membrane proteins.[38,40,41] Validation of and sampling in such systems are computationally highly demanding because of composite nature of the phospholipids.[32,47] Herein, we employ the dynamic refinement approach making use of a simplified membrane system, vide infra.

To the best of our knowledge, neither the sodium-chloride dependent transporter structure LeuT, nor a homology model derived thereof (hSERT), have been studied by simulation methods. Here, we report MD simulations of the Na^+/Cl^--dependent transporters LeuT and hSERT in a membrane system to address ligand-binding modes and binding site flexibility. We used LeuT as a template for constructing a hSERT homology model structure.[48] In the modeling procedure, information from experimental mutagenesis data on the transporters has been used.[21,22,49] To verify our membrane system, we have included LeuT in our study. We tested our model system by comparing atomic fluctuations (extracted from MD simulations) with those derived from the crystallographic B factors and by monitoring the stability of key interactions during the simulations. We then used the same methodology to study hSERT in complex with either serotonin (5-HT, natural substrate) or escitalopram (SSRI/allosteric serotonin reuptake inhibitor) to investigate the flexibility of the binding site and to determine key protein–ligand interactions.

Results and Discussion

Knowledge of the three-dimensional (3D) structure of proteins is a prerequisite for understanding their function. In the absence of experimental structural data, comparative modeling of proteins is a possible alternative to obtain structural information. Based on the template LeuT, we built a 3D model for hSERT[48] and used this model to study the possible binding mechanisms of the natural substrate 5-HT and the highly active inhibitor, escitalopram.

Homology modeling of the serotonin transporter and introduction of ligands

A detailed description on the homology modeling step is described by Jørgensen et al.[48] and, therefore, only a short description is provided here. Based on the alignment of hSERT to the LeuT structure (shown in the Supporting Information), an initial homology model of the hSERT apo protein was constructed. Initial attempts to dock serotonin into this model revealed that there was not enough space for this endogenous ligand. Docking escitalopram into the site was even more problematic. As the residues in the unwound regions of transmembrane domains TM1 and 6 are not conserved among the NSS transporters, the structure of these regions could be expected to vary between these transporters. Backbone flexibility was therefore allowed in these regions, along with some flexibility of TM3 and 8, to allow for the movements of TM1 and 6.[48] Some parts of TM6 moved closer towards the four surrounding transmembrane domains: TM2, 5, 7, and 11. These adjacent regions were kept in space during model construction. After additional manual side-chain reorientations (most were unfavorable according to a rotamer library[50]), escitalopram in its proposed bioactive conformation[8] could be introduced into the putative binding cleft. By mutating residues that are not conserved between LeuT and hSERT in the ligand-binding site to alanine or glycine and using this modified ligand-bound structure as template in a second step of homology modeling, models with alternative structural organizations of the binding site were obtained.[48] In the final escitalopram-bound hSERT model, we observed slightly different backbone conformations of TM1, 3, 6, and 8 compared to LeuT and different intramolecular protein–protein contacts. To test this escitalopram-optimized model, we introduced 5-HT in the binding site (docked manually using two out of three pharmacophore elements from the SSRI pharmacophore model, namely the amine lone pair and the centroid of the aromatic part of the cyanophthalane group. This docking pose gave rise to protein–ligand interactions as proposed in a 5-HT pharmacophore model.[8–14] In the obtained binding mode, 5-HT was in contact with several residues experimentally proven to be important for substrate binding, for example, D98, I172, and Y176[51–54], cf. Figure 1a. If the model could relax into a conformation suitable for 5-HT-binding during MD simulations, the constructed model could be considered reliable.

Construction of the transporter-model membrane-solvent system

Membrane-embedded proteins are in contact with at least three physically diverse environments; the intra- and extracellular fluid, in which the protein terminals and the loop regions that connect the TMs are located; the hydrophobic region of the membrane, facing large parts of the protein surface; and the charged head groups of the phospholipids located at the interfacial regions between the membrane and the aqueous solutions. We could have chosen a detailed description of a phospholipid membrane, but such systems are computational-

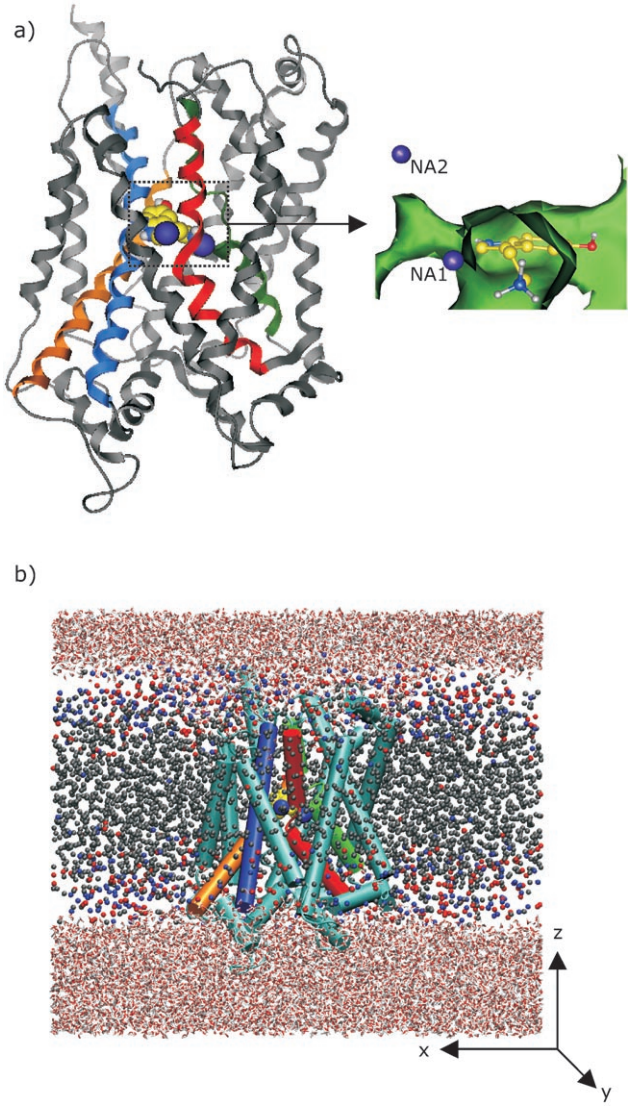

Figure 1. Homology model of hSERT-5-HT before MD simulations. The protein is shown as ribbon: TM1, 3, 6, and 8 are highlighted in red, orange, green, and blue, respectively. Serotonin and the two sodium ions are highlighted in yellow and blue, respectively. a) Front view. For clarity, the protein orientation in the insert is different from the main figure. b) Front view of the simulation system after equilibration. Membrane atoms are displayed as van der Waals sphere and colored in grey (neutral), blue (positively charged) and red (negatively charged). Water molecules are displayed in stick representation.

ly highly demanding.[32] Instead, we used a simplified system that in a proper manner contains the essential membrane characteristics. The methods employed to construct the membrane system are described in detail in the experimental section along with the simulation strategy.

Three different systems were considered: 1) the *A. aeolicus* leucine transporter with its endogenous ligand,[18] 2) the 5-HT-bound serotonin transporter, and 3) the escitalopram–serotonin transporter complex. Coordinates for LeuT were obtained from the Protein Data Bank (accession code 2A65),[55] whereas the protein structures of hSERT were constructed by homology modeling.[48] The final systems consisted of 43 000–45 000 atoms and were organized as shown in Figure 1 b.

Overall structures

In the LeuT structure, the leucine ligand and two sodium ions, NA1 and NA2, are located between the four transmembrane domains, TM1, 3, 6, and 8 (these four regions are highlighted in the hSERT model shown in Figure 1).[18] Notably, in the LeuT X-ray structure, none of these helical domains have ideal helix forms: TM1 and 6 are unwound in the middle, whereas TM3 and 8 are bent and lack one or more hydrogen bonds compared to the ideal helices.[56] This nonideal topology/geometry seems important for providing room for a ligand. It offers multiple protein–ligand interactions, involving backbone and side-chain atoms, and induces required conformational changes during the transport cycle.[18] Most residues contributing to this structural organization are conserved between the transporters, but heterogeneity is observed particularly in the network tightening these regions together. These differences might be linked to the ability of transporters to discriminate between various substrates and inhibitors and, consequently, variations in the tertiary structure in the active site can be expected. Figure 1 a shows how 5-HT and two sodium ions, NA1 and NA2, are located in the corresponding binding cleft in the hSERT model. This overall organization was maintained throughout the simulation. For the hSERT–escitalopram model, a similar arrangement was found before and after the simulation (data not shown).

We initially investigated changes in the overall structure of the LeuT- and 5-HT-bound hSERT during the simulations. For LeuT, the membrane-embedded part was hardly affected by the simulations, whereas some of the loop regions underwent slight conformational changes (data not shown). This was not surprising and in agreement with other studies in which model protein structures originally constructed in vacuo have been examined in a composite water-membrane environment.[26,29,57] In both hSERT–ligand models, a similar structural rearrangement was observed in the loop regions (data not shown). Additional conformational changes were found in TM2, 3, 5, 6, 7, 8, and 11. Notably, four of these regions, TM2, 5, 7, and 11, surrounded TM6. During the simulation, TM2, 5, 7, and 11 seemed to adopt more favorable conformations that in addition allowed for a more relaxed conformation of the TM6 coil region. Using HELANAL[56] to characterize the α helix geometry, we found that in LeuT and in the initial hSERT models, TM3 is bent $24 \pm 10^{\circ}$ around residues Y107 (LeuT)/Y175 (hSERT). During the simulation, TM3 in hSERT adopted a straighter conformation (bending angle $6.6 \pm 1.7^{\circ}$ (5-HT) or $8.0 \pm 14.3^{\circ}$ (escitalopram)) than in LeuT, and part of it (residues hSERT 175–193) rotated about 30° around its own axis, whereas the bending was maintained in LeuT. Superimposing TM3 in 5-HT-bound hSERT after the simulation with TM3 in the LeuT X-ray structure (only C_{α} atoms included in superimposition) gave a root-mean-square deviation (rmsd) of 2.66 Å; the corresponding value for the rotated part of TM3 was 0.82 Å. In the hSERT model, these

changes seemed to be necessary to accommodate the different ligands.

To examine the temporal conformational variations of the transporters within the membrane system during the MD simulations, the time evolution of the root-mean-square deviation of the atomic positions was calculated for each complex (Supporting Information). Rmsd for the entire protein increased slightly over time because of movements restricted to solvent-exposed loop regions, whereas residues in the ligand-binding site reached an equilibrium state. In all three transporter–ligand complexes, an equilibrium state was obtained for the ligand-binding cleft after about 2 ns (rmsd ~0.7–0.9 Å), whereas the membrane spanning regions TM1–11 equilibrated after about 4 ns. Overall, the fluctuations suggested that the topology of the LeuT structure and hSERT models were stable.

Fluctuations of individual residues along the polypeptide chains after equilibration were investigated by examining rmsd for the Cα atom of each residue. The fluctuations of LeuT were compared to rmsd ($\langle x^2 \rangle$) derived from the crystallographic B factor,[18] cf. $B = 8\pi\langle x^2 \rangle$.[58] Figure 2a shows that the fluctuations observed in LeuT during MD simulations were in good agreement with the crystallographic B factors. Similar fluctuations were observed in hSERT (Figure 2b). In both proteins, the membrane spanning regions and the loop regions had different dynamic behavior. Average fluctuations of about 0.8 Å were found for the 12 TM domains, whereas the terminals and intra- and extracellular loop regions had rmsd fluctuations in the range of ~0.8 to ~8 Å. In fact, the most pronounced fluctuations were observed for the extracellular regions EC2, EC3, and EC6 regions, which were exposed to the aqueous phase, whereas the binding cleft showed relatively little flexibility in both proteins, cf. Figure 2.

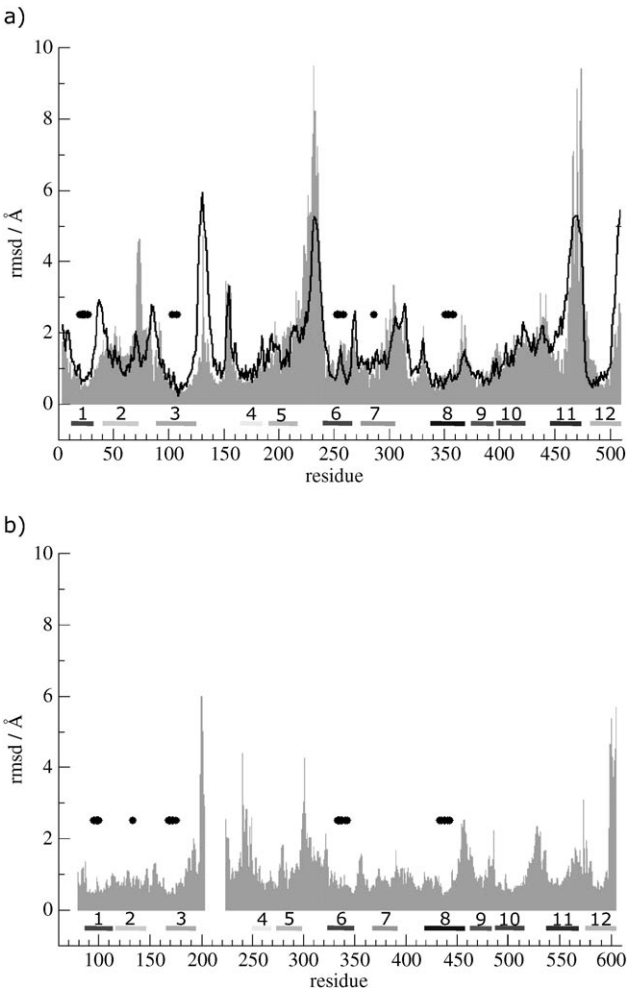

Figure 2. Residue-by-residue Cα root mean square deviations (rmsd) compared to the initial positions obtained after equilibration. a) Rmsd for LeuT. Molecular dynamics simulation results (rose bars) are compared with the rmsd derived from the crystallographic *B* factors (black line). b) Rmsd for the 5-HT-bound hSERT model extracted from the simulation. The bars indicate the position of the 12 transmembrane domains. The regions indicated by black dots are located within 7 Å of the substrate. The initial ~3 ns of each trajectory was considered as equilibration and discarded for analysis. The gap corresponds to residues 204–233 that make up a long extracellular loop region for which no template structure is available. The N- and C-terminals are also much longer in hSERT than in LeuT. For these reasons, the residues were not included in our model.

Protein–sodium interactions

Proteins within the neurotransmitter:sodium symporter family mediate the transport of neurotransmitter substrates across the cell membrane by using the naturally occurring neuronal sodium gradient as driving force. Consequently, the ability to bind sodium is likely to be conserved among the NSS transporters. In the LeuT X-ray structure, two sodium ions, NA1 and NA2, were identified, cf. Figure 3a and b. These are located in close vicinity of the leucine ligand. NA1 is coordinated by six ligands (the leucine ligand (O) as well as residues A22(O), N27(Oδ), T254(O and Oγ), and N286(Oδ)) in an octahedral coordination sphere in the X-ray structure[18] and maintained during the simulation (Figure 3a). Note that Protein Data Bank (PDB) nomenclature is used throughout the discussion. NA2 is faced by five ligands (G20(O), V23(O), T354(Oγ), S355(Oγ), and A351(O)) organized in a bipyrimidal trigonal fashion (Figure 3b) in the X-ray structure,[18] and this coordination is maintained throughout the simulation. In our hSERT model, only five residues (D98(Oδ), A96(O), N101(Oδ), S336(O), and F335(O)) coordinate NA1 in a bipyrimidal trigonal coordination sphere, cf. Figure 3c. This is slightly different from the corresponding site in LeuT; hSERT D98(Oδ) has replaced the LeuT leucine ligand(O) atom, T254(Oγ) is replaced by hSERT F335(O), whereas the hSERT counterpart to LeuT N286, residue hSERT N368 is not involved in NA1-binding (NA1 to N368(Oδ) distance is ~5.4 Å, not shown). Most of the residues that surround hSERT N368 are not conserved between hSERT and LeuT transporters, for example, hSERT T364 corresponds to A282 in LeuT, hSERT V367 to L287 in LeuT, hSERT C369 to E287 in LeuT, and hSERT T371 to A289 in LeuT. Consequently, the hydrogen-bonding network around N368/N286 differs between hSERT and LeuT, which gives rise to different conformations of the residues involved in both transporters, suggesting different roles of the asparagines in different transporters. As shown in Figure 3d, the NA2 site in hSERT involves residues G94(O), V97(O), D437(both Oδs), and S438(Oγ). D437 (T354 in LeuT) do-

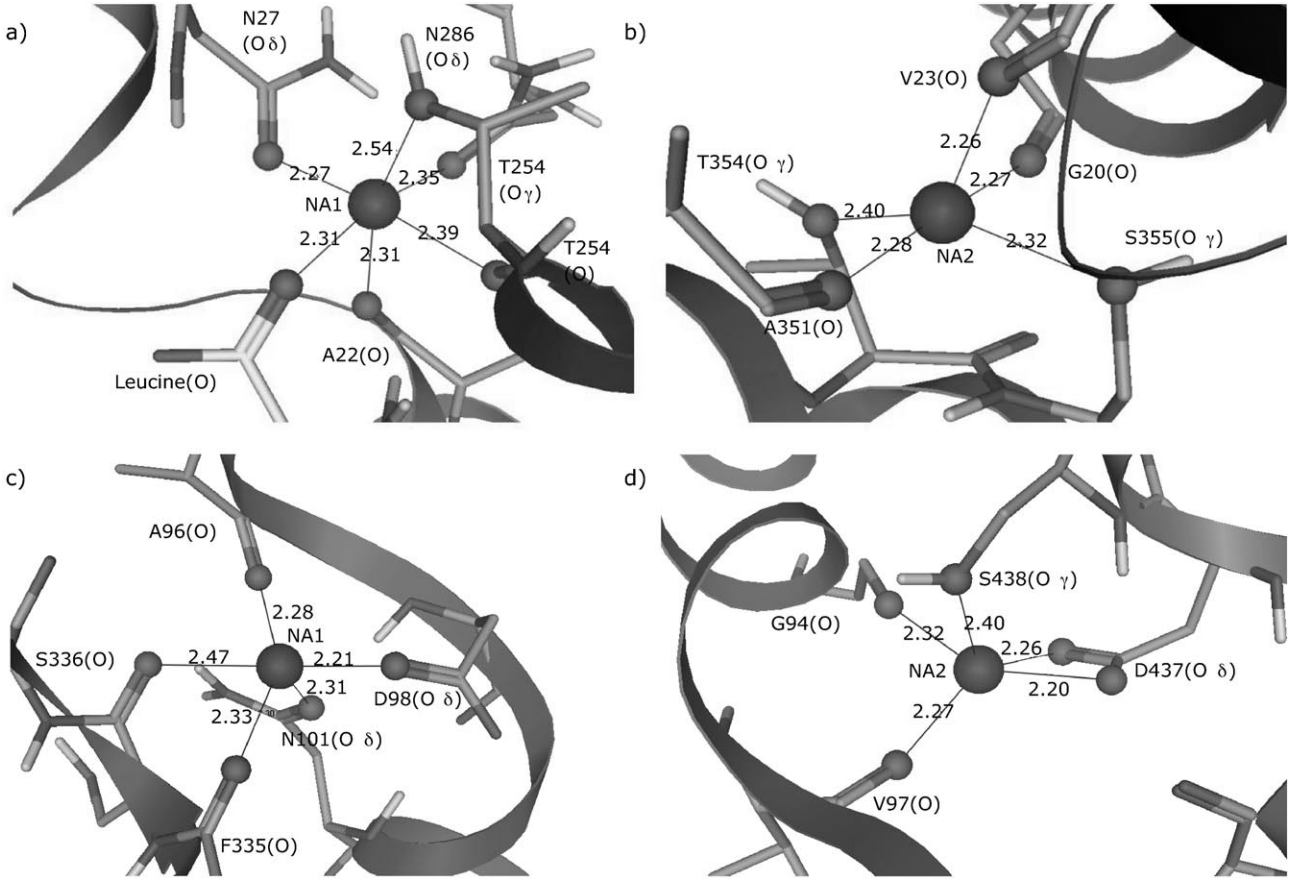

Figure 3. The sodium-binding sites in the transporters. a) NA1 in LeuT. b) NA2 in LeuT. c) NA1 in 5-HT-bound hSERT. d) NA2 in 5-HT-bound hSERT. Mean distances (Å) extracted from the simulations are indicated. For clarity, the orientation differs between LeuT and hSERT.

nates both of its carboxylate oxygens to the NA2, thereby replacing the fifth residue, LeuT A351 (hSERT L434) which in LeuT coordinates NA2 (Figure 3b). To the best of our knowledge, no mutagenesis studies have been performed for LeuT, whereas some of the residues involved in sodium binding in our hSERT model have been found to be important for sodium binding and/or transporter function, for example, A96, D98, and N101.[53,59–61]

In addition to their function for ion translocation, the two sodium-binding sites contribute to structural stability in the proteins. Tight coordination of sodium ions in both proteins would therefore be expected. We investigated the stability of the sodium pockets in the LeuT structure and in the homology model by analyzing the variations in sodium–protein contacts during the MD simulations. The average fluctuations in contacts between NA1/NA2 and the coordinating atoms in both proteins are listed in Tables 1–3. We found that the bond lengths in NA1 and NA2 in LeuT, 5-HT-bound hSERT, and escitalopram-bound hSERT are stable and maintained throughout the simulations (data available in the Supporting Information).

Table 1. Mean distances and standard deviations of selected distances in LeuT extracted from MD simulations.[a]

Contact	Mean distance ± standard deviation (Å)
NA1-LEU(O)	2.3 ± 0.1
NA1-N27(Oδ)	2.3 ± 0.1
NA1-T254(Oγ)	2.4 ± 0.1
NA1-T254(O)	2.4 ± 0.1
NA1-N286(Oδ)	2.5 ± 0.2
NA1-A22(O)	2.3 ± 0.1
NA2-A351(O)	2.3 ± 0.1
NA2-S355(Oγ)	2.3 ± 0.1
NA2-T354(Oγ)	2.4 ± 0.1
NA2-G20(O)	2.3 ± 0.2
NA2-V23(O)	2.3 ± 0.1
LEU(O)-Y108(OH)	2.7 ± 0.2
LEU(O)-G24(N)	3.9 ± 0.2
LEU(O)-L25(HN)	2.9 ± 0.3
LEU(O)-G26(N)	2.8 ± 0.1
LEU(N)-F253(O)	2.8 ± 0.1
LEU(N)-T254(O)	3.0 ± 0.2
LEU(N)-S256(Oγ)	2.8 ± 0.1
LEU(N)-N21(O)	3.3 ± 0.2
S256(Hγ)-N21(Oδ)	1.9 ± 0.2
S256(Hγ)-N21(O)	2.7 ± 0.2

[a] LEU refers to the ligand, leucine.

Protein–ligand interactions

Leucine in LeuT. The leucine-binding site is composed of a polar and a hydrophobic region, and both regions are occu-

Table 2. Mean distances and standard deviations of selected distances in 5-HT-bound hSERT calculated from MD simulations.

Contact	Mean distance ± standard deviation (Å)
NA1-D98(Oδ)	2.2 ± 0.2
NA1-N101(Oδ)	2.3 ± 0.1
NA1-L337(O)	4.1 ± 0.5
NA1-S336(O)	2.5 ± 0.3
NA1-F335(O)	2.3 ± 0.2
NA1-A96(O)	2.9 ± 0.1
NA2-L434(O)	4.4 ± 0.5
NA2-S438(Oγ)	2.4 ± 0.1
NA2-D437(Oδ1)	2.3 ± 0.1
NA2-D437(Oδ2)	2.2 ± 0.1
NA2-G94(O)	2.3 ± 0.1
NA2-V97(O)	2.3 ± 0.1
5-HT(amine N)-D98(Oδ)	3.0 ± 0.5
5-HT(amine N)-Y95(O)	4 ± 1
5-HT(amine N)-L337(O)	3.9 ± 0.9
5-HT(indole NH)-T439(Oγ)	2.5 ± 0.7
5-HT(indole OH)-G442(O)	3 ± 1
Y95(HH)-G338(O)	2.4 ± 0.7
Y95(O)-S438(Hγ)	3 ± 1
D98(Oδ)-Y176(OH)	2.1 ± 0.9
D98(Oδ)-Y176(HH)	1.9 ± 0.7
L99(HN)-Y176(OH)	3.9 ± 0.5
Y175(HH)-E493(Oε)	3.1 ± 0.9
Y176(HH)-D437(Cγ)	9.5 ± 0.6
Y176(HH)-S438(Oγ)	6.5 ± 0.7
Y176(OH)-S438(Hγ)	7.1 ± 0.7
L434(O)-S438(Hγ)	5 ± 1
G435(O)-T439(Hγ1)	1.8 ± 0.2
D437(Cγ)-S438(Hγ)	4.6 ± 0.7
S438(O)-G442(HN)	2.1 ± 0.4

Table 3. Mean distances and standard deviations of selected distances in escitalopram-bound hSERT calculated from MD simulations.

Contact	Mean distance ± standard deviation (Å)
NA1-D98 (Oδ)	2.3 ± 0.1
NA1-N101 (Oδ)	2.3 ± 0.1
NA1-L337 (O)	4.8 ± 0.3
NA1-S336 (O)	2.3 ± 0.1
NA1-F335 (O)	2.5 ± 0.2
NA1-A96 (O)	2.4 ± 0.2
NA2-L434 (O)	6.4 ± 0.3
NA2-S438 (Oγ)	4 ± 1
NA2-D437 (Oδ1)	2.3 ± 0.1
NA2-D437 (Oδ2)	2.2 ± 0.1
NA2-G94 (O)	2.2 ± 0.1
NA2 V97 (O)	2.2 ± 0.1
ESC(N″)-D98(Oδ)[a]	2.7 ± 0.1
ESC(N″)-Y95(O)[a]	4.4 ± 0.3
ESC(N″)-L337(O)[a]	5.1 ± 0.6
D98(Oδ)-Y176(OH)	5.2 ± 0.4
D98(Oδ)-Y176(HH)	5.4 ± 0.8
Y176(HH)-S438(Oγ)	3.3 ± 0.7
Y176(OH)-S438(Hγ)	3.5 ± 0.4
G338(O)-Y95(HH)	3 ± 1
S438(Hγ)-Y95(O)	3 ± 1
S438(Hγ)-L434(O)	4.1 ± 0.4
S438(Hγ)-D437(Cγ)	4.1 ± 0.4
T439(Hγ1)-G435(O)	4.8 ± 0.5

[a] ESC refers to escitalopram.

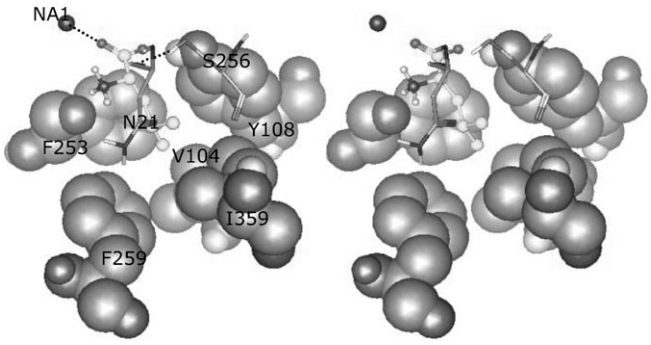

Figure 4. Stereoview of the hydrophobic part of the leucine-binding site in LeuT obtained after simulation. Residue S355 is not shown for clarity.

pied by the polar head group of the leucine ligand and the hydrophobic side chain, respectively.[18] The hydrophobic part of the binding site is shown in Figure 4. The conformation corresponds to the last frame of the MD simulation. As summarized in Table 4, polar and hydrophobic parts of the ligand establish contacts with the protein. These contacts are stable and only minor fluctuations are observed throughout the simulations (Table 1 and additional data are provided in the Supporting Information). The formation of a hydrogen bond between N21 and S256 seems important for keeping the TM1 and TM6 coil regions together, thereby stabilizing the active site in a conformation suitable for leucine binding. Interestingly, we observed that the hydrogen-bonding networks between the ligand carboxyl group and residues A351, Y108, S355, and N21 flip back and forth between two organizations, networks 1 and 2, mediated by rotations of the Y108 and S355 hydroxyl groups (Figure 5a and b). In network 1, S355 functions as hydrogen donor in a hydrogen-bonding contact between the side chain of this residue and the main-chain carbonyl oxygen from N21 (Figure 5a), whereas in the other network, S355 forms a hydrogen bond with the Y108 side-chain hydroxyl group (Figure 5b). Analogously, the Y108 hydroxyl group forms a hydrogen bond to the substrate as described above in network 1, whereas its proton points toward the backbone carbonyl oxygen of A351 in network 2. In summary, all essential interactions found in the LeuT X-ray structure are maintained during the simulation,

Table 4. LeuT–leucine interactions monitored in the MD simulation.

Leucine	Type of interactions	Residues involved in LeuT
carboxyl group	hydrogen bonding/ electrostatic interactions	amide nitrogen of L25, G26; hydroxyl group of Y108, NA1
amino group	hydrogen bonding/ electrostatic interactions	carbonyl backbone oxygens of N21, F253, T254; hydroxyl group of S256
methyl groups	hydrophobic interactions	V104, F253, I359

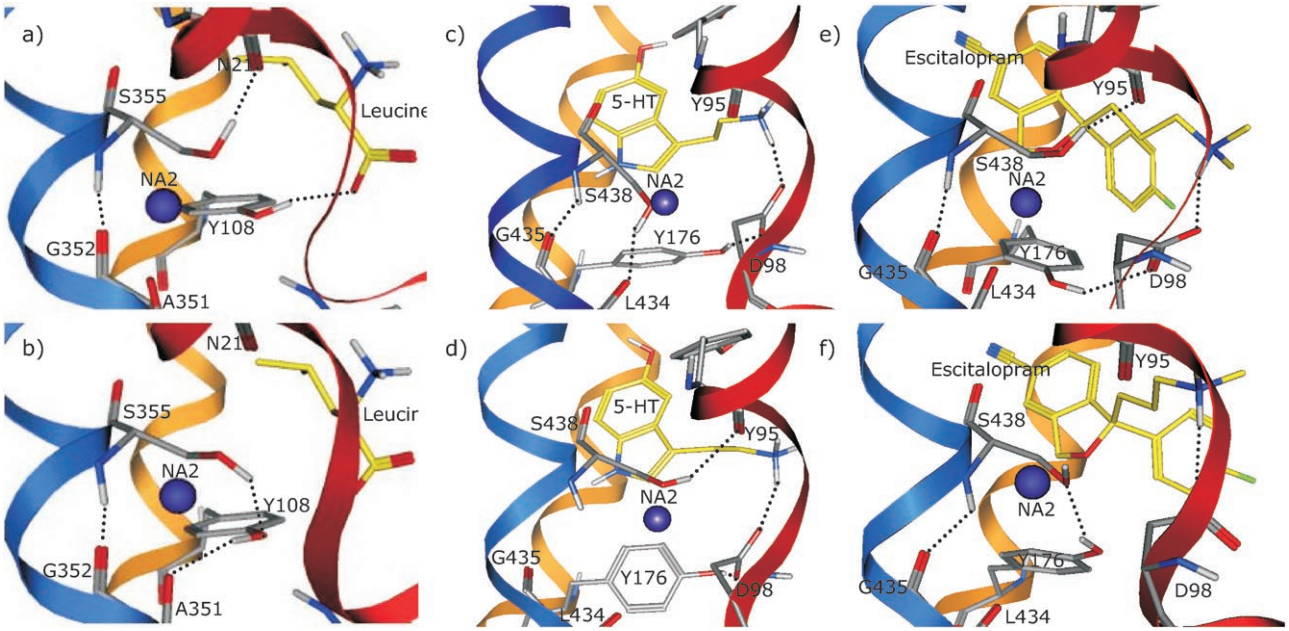

Figure 5. Hydrogen-bonding network in LeuT and hSERT. a) Network 1 in LeuT. b) Network 2 in LeuT. c) Network 1 in 5-HT-bound hSERT. d) Network 2 in 5-HT-bound hSERT. e) Network 1 in escitalopram-bound hSERT. f) Network 2 in escitalopram-bound hSERT. Network 2 dominates in the hSERT-inhibitor complex.

indicating that our membrane system appears sufficient to capture the essential protein dynamics.

5-HT in hSERT. 5-HT occupies two subpockets within the active site: A relatively wide hydrophobic part into which the indole skeleton is located, and a narrow funnel occupied by the ethylamino group. NA1 and D98 are located at the end of this funnel, cf. Figure 6. Protein–protein and protein–ligand

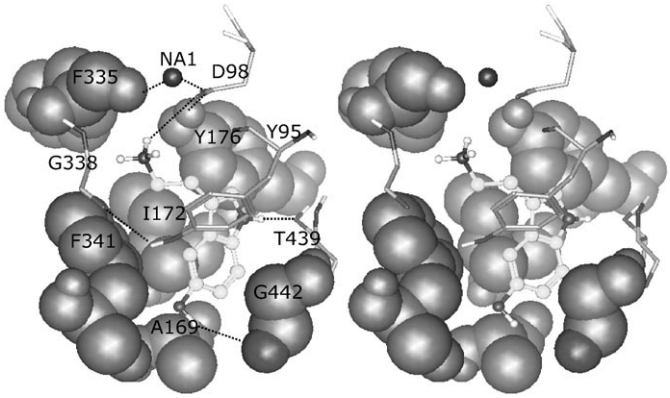

Figure 6. Stereoview of the 5-HT-binding site in hSERT obtained after simulation.

contacts of the narrow subpocket are stable, and only relatively small fluctuations in distances between selected residues are observed (Table 2). During the simulation, protein–ligand contacts in the hydrophobic pocket change. The substrate reorients slightly, such that new contacts between the indole part of the ligand and the binding cleft are established, vide infra. In the following, a detailed description of protein–ligand interactions is provided.

One of the D98 carboxyl oxygens is involved in a combined hydrogen bond/salt bridge with the protonated ligand nitrogen as proposed from mutagenesis and pharmacophore modeling studies.[9,53] The other D98 carboxyl oxygen forms hydrogen bonds with the Y176 hydroxyl group (Figure 7b) and to G100 (data not shown) and functions as axial ligand to NA1 (Figure 6). A mutational study has revealed that a D98E mutant binds gramine, a shorter substrate analogue, but cannot couple the transport of gramine to the sodium gradient.[53] This indicates that residue D98 is involved in sodium and ligand-binding as observed in our model. At the binding site, two interhelical contacts keep TM1 and TM3 (D98(Oδ) to Y176(HH)), and TM1 and TM6 (Y95(HH) to G338(O)) together, respectively. Figure 7b and c show that these contacts are maintained throughout the simulation although some fluctuations in contact distances are observed. Interestingly, we observed that during the 1.5 ns of MD simulation, where Y176 is not involved in hydrogen-bonding to D98, it is instead in contact with a water molecule. This water molecule is one of the crystal waters present in LeuT[18] and was introduced in the corresponding position in the hSERT model. In addition to the ionic contact with D98, the ligand amine establishes alternately hydrogen bonds to Y95(O) and L337(O), cf. Figure 7d–f. In the initial binding mode, the indole hydroxyl group interacts with the A169 carbonyl, whereas the proton at the indole nitrogen points towards the centre of the Y176 aromatic part (data not shown). Shortly after initiation of the simulation, the substrate reorients, and electrostatic interactions are established between the 5-HT indole hydroxyl group and the main chain oxygen of G442 and between the proton at the indole nitrogen and the hydroxyl group of residue T439 (Figure 6 and 7g–h). The distance between the ligand hydrogen involved and the carbonyl group of the protein is on the borderline of

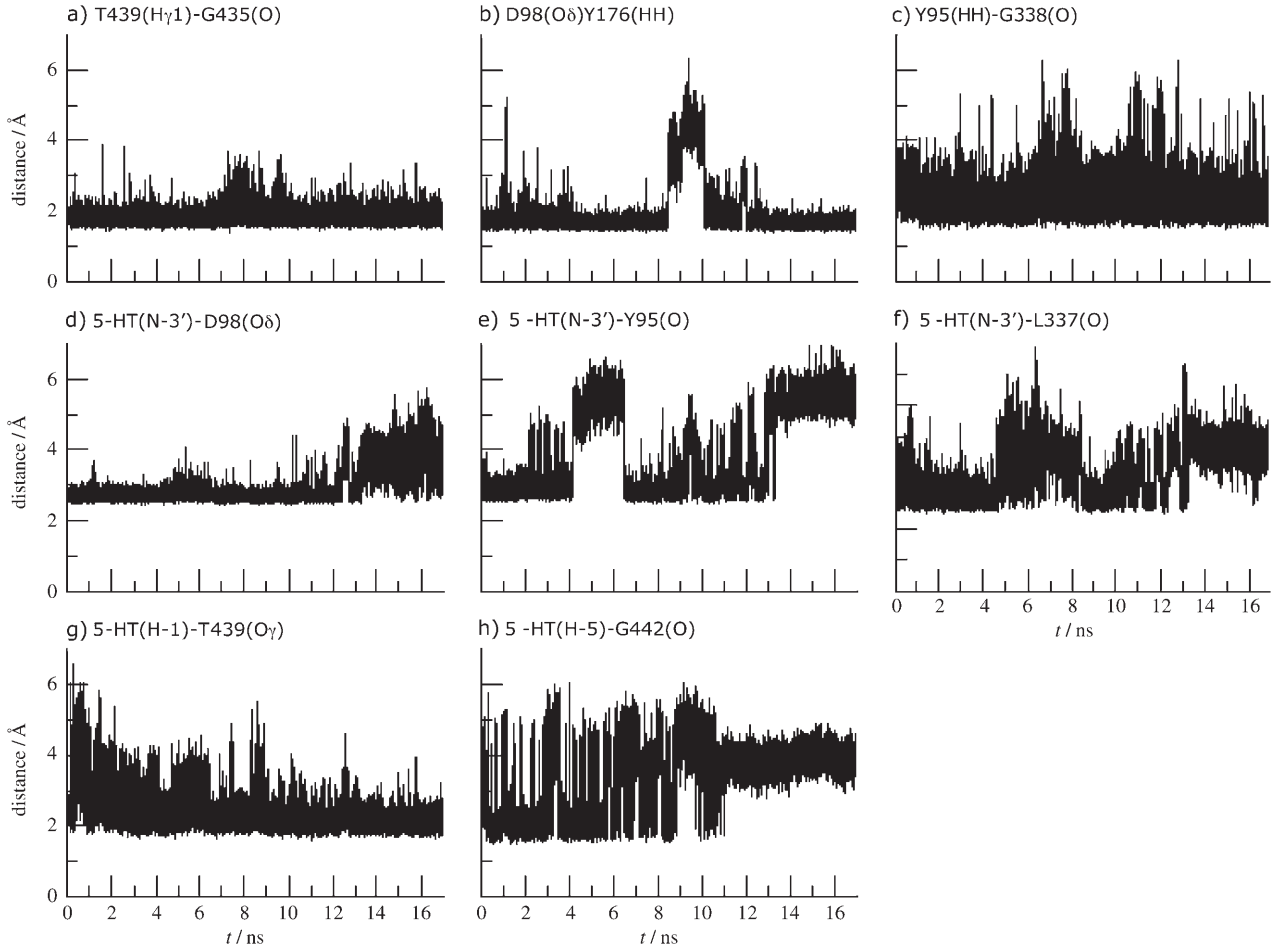

Figure 7. Time evolution of distances between selected atoms in 5-HT-bound hSERT monitored during MD simulations. a)–c) Distances between atoms of selected residues as indicated by insets. d)–h) Distances between atoms in 5-HT and selected residues of hSERT as indicated by insets. The atom numbers in 5-HT refer to the numbering Scheme in the Insert showing the chemical structures.

where the formation of a direct hydrogen-bond is possible[62] and as a consequence, the distances between 5-HT and those two residues vary during the simulation. Initially, hydrogen-bonding to G442 dominates, which weakens during the simulation (Figure 7h) and a complementary interaction between the indole nitrogen proton and T439 is stabilized (Figure 7g). We observed that the conformation of the T439 side chain is stabilized by a hydrogen bond between the T439 hydroxyl group and the G435 main chain oxygen atom, cf. Figure 7a. Only small fluctuations are observed, suggesting that the changes in the contacts between 5-HT, G442, and T439 are due to variations in the 5-HT orientation. In addition, residue I172 interacts with the substrate through hydrophobic interactions with the indole skeleton. Based on site-directed mutagenesis studies, it has also been suggested that I172 is directly involved in the ligand-binding site.[9,51]

Comparing the protein–ligand interactions with the predictions from pharmacophore modeling reveals that both binding modes are in agreement with Pratuangdejkul and co-workers' hypothesis.[9] Based on 3D-QSAR modeling of 121 5-HT analogues, the authors propose four protein–ligand interactions: 1) electrostatic contacts between the amine nitrogen and the protein, 2) hydrogen bond between the hydroxyl group (hydrogen donor) and the protein, 3) hydrophobic interactions between the indole ring system and the protein, and 4) polar interaction between the indole ring system and the protein, either by cation π or polarized aromatic–aromatic interactions. The authors could not deduce the explicit role of the indole nitrogen and its proton. The nitrogen could play a major role in the electron distribution throughout the indole ring orbitals and/or function as a hydrogen donor.[9] In our simulation, we can observe these proposed interactions: D98–amine electrostatic interaction, G442 5-HT hydroxyl–hydrogen bond, hydrophobic contacts between I172 and 5-HT, and electrostatic contact between T439 and the indole nitrogen proton. Overall, the analysis of the molecular dynamics simulations of the hSERT-5-HT complex confirmed that the escitalopram-optimized hSERT homology model could relax into a conformation suitable for the binding of the natural substrate of the transporter.

Escitalopram in hSERT. As shown in Figure 8a, the three components of escitalopram, the dimethylaminopropyl chain, the fluorophenyl group, and the cyanophthalane skeleton occupy separate subpockets in the protein. The subpocket occupied by the indole skeleton of 5-HT corresponds to the sub-

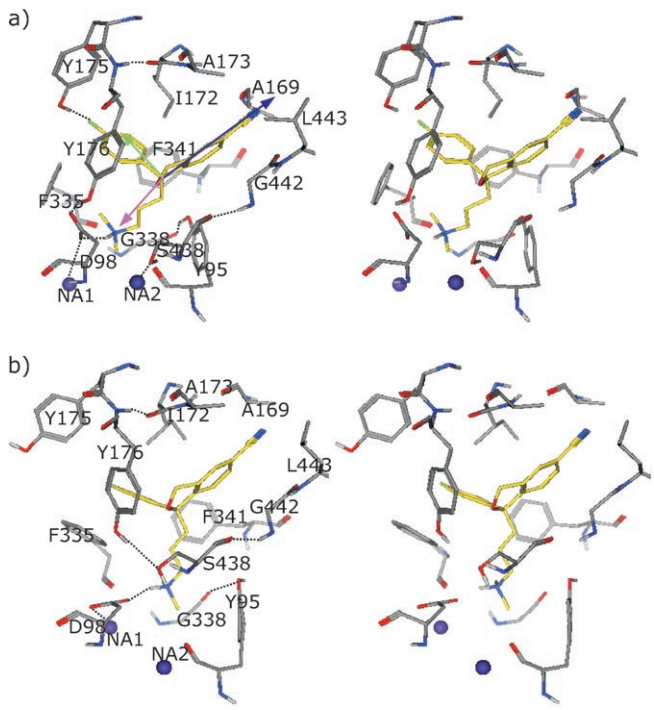

Figure 8. Stereoview of the escitalopram-binding site in hSERT. a) Initial homology model. The three arrows indicate the three different sub-pockets occupied by the ligand: cyanophthalane (blue), fluorophenyl (green) and dimethylaminopropyl (purple). b) After 7 ns of MD simulation.

pocket occupied by the cyanophthalane skeleton, whereas the narrow funnel-like pocket occupied by the ethylamine side chain of 5-HT shares similarities with the dimethylaminopropyl pocket. In the initial model (Figure 8a), we observed the following interactions in the binding site: the dimethylaminopropyl chain interacts with the protein by a ligand-amine to the D98 salt bridge and by a number of hydrophobic contacts, including an interaction between one of the methyl groups of the ligand amine and the F335 phenyl ring, and contacts between the ligand propyl chain and the aromatic rings of Y95 and F341. The fluorophenyl ligand part is in contact with the side chains of Y176, F341, and I172 (hydrophobic contacts/π-π stacking between the side chains of these residues and the aromatic moiety of the ligand) and its fluorine interacts with residue Y175. Residues A169 and G442, and the δ-methyl group of residue I172 face the cyanophthalane moiety.[48] The observed protein–ligand interactions are in good agreement with predictions from mutagenesis studies suggesting interactions between escitalopram and residues D98, Y95, A169, and I172.[53,54,63]

During the MD simulations, we observed that one of the interhelical contacts changed. A TM3–TM8 contact (between Y176(HH) and S438(Oγ)) mediated by a rotation of the Y176 side chain and a slight conformational change in S438 replaced the TM1–TM3 contact between D98 and Y176. As shown in Figure 5e and f, this change gave rise to a replacement of a protein–protein contact across the middle of the ligand-binding site with a protein–protein contact, only transversing one side of the binding pocket. This change increased the volume available for ligand binding compared to the binding site in the hSERT–5-HT complex. Taking into account the larger size of this inhibitor compared to the natural substrate, these changes seemed necessary for inhibitor binding (Figure 9). From time to time, the new contact was stabilized by an additional hydrogen bond between S438 and D437 (Figure 9l). An interhelical contact between Y176(OH) and L99(HN) was also formed and maintained throughout most of the 7 ns of the MD simulation (Figure 9f). This contact was also likely to contribute to a stabilization of the escitalopram-binding site. Comparing these protein–protein interactions with those in the 5-HT-binding site revealed that different contacts dominated in the two complexes throughout the simulation. In the case of 5-HT, residue Y176 was involved in hydrogen-bonding to D98 (Figure 9a), as would also be expected according to the LeuT X-ray structure (see Supporting Information). On the other hand, in the hSERT–escitalopram complex, Y176 interacted with S438 and L99 (Figure 9d and f). In the hSERT–5-HT complex, S438 was alternately hydrogen-bonding to Y95 and L434 (Figure 9g and i), whereas this residue primarily interacted with Y176 and D437 (Figure 9d and l) in the hSERT–escitalopram complex. Interactions in the hSERT–substrate complex shared similarities with the contacts in the LeuT substrate complex. This was observed by comparing contacts in LeuT with corresponding contacts in hSERT–5-HT. We compared the contact between Y108 and the leucine ligand, and the contact between S355 and N21 in LeuT (Figure 5a), with the contacts between Y176 and D98, and between S438 and Y95 in hSERT–5-HT (Figure 5d). Our results indicated that different sets of interactions dominated in the binding cleft when a substrate or an uptake inhibitor was bound. Such conformational changes induced by ligand binding are considered "induced fit" according to the induced fit hypothesis.[64,65] The induced fit mechanism is commonly observed and, for instance, has been proposed for ligand binding to P-glycoproteins and transferase.[66,67] For these proteins, size and shape of the ligands induce conformational changes to either accommodate a broad range of substrates[67] or trap the protein in a conformational state that is inaccessible for the substrate.[66] Such structural alterations may be an attractive approach for designing small molecules specifically targeting the conformational changes required for substrate transport; that is, trapping the transporter in a state that obstructs the substrate transport. It remains to be proven whether the escitalopram-induced conformational changes observed during the simulation interfere with the conformational changes occurring during the transport of the natural substrate.

The conformation of Y176 obtained after the hSERT–escitalopram simulation allows for hydrophobic interactions between the side chain of this residue and the ligand fluorophenyl group. During the simulation, we also observed that the side chains of residues I172, Y175, and F335 changed orientation. The side chain of I172 reorientates but interacts throughout the simulation with the aromatic rings of escitalopram by multiple hydrophobic contacts. The side chain of residue Y175 rotates away from the binding cleft so that the initial interaction between its hydroxyl group and the fluorine atom in the ligand is lost. In this position, it interacts with E493 in the

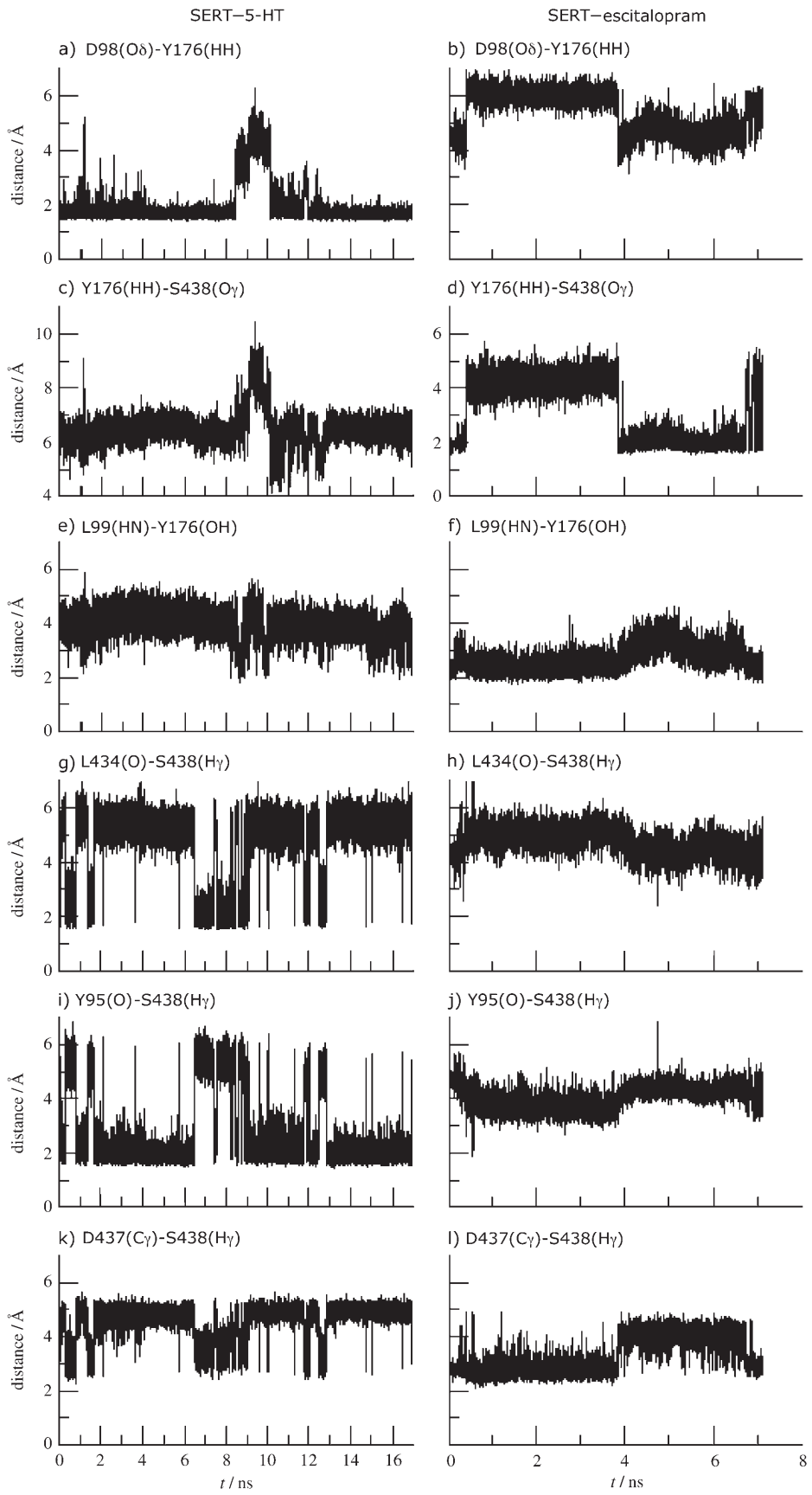

Figure 9. Time evolution of distances between atoms of selected residues (indicated by the insets) in 5-HT-bound hSERT (left column) and escitalopram-bound hSERT (right column) monitored during MD simulations.

same way as observed in the hSERT–5-HT complex and the LeuT X-ray structure (LeuT D404). The aromatic moiety of residue F335 flips 90° around its own axis to form parallel displaced π-π stacking[68,69] with the ligand fluorophenyl group. Additionally, we observed a slight movement of escitalopram. In the new position, a π-π interaction between F341 and the escitalopram fluorophenyl group replaced the initial interaction between F341 and the dimethylaminopropyl side chain. These contacts were maintained during the remaining part of the simulation. We observed that the π-π stacking interactions between the aromatic rings of the protein and the ligand in general were optimized, so that these interactions, along with the salt bridge between the ligand amine group and the side chain of D98, dominated the protein–ligand contacts. Rotations of I172 during the simulation also gave rise to a strengthening of the contacts between this side chain and aromatic moieties of escitalopram. In fact, the conformation of I172 in the final frame (Figure 8b) was one of the most populated in a rotamer library.[50] In this conformation, numerous atoms of I172 and the ligand interacted by hydrophobic interactions (C(δ)–C-6 distance 3.8 Å; C(δ)–C-7 distance 3.5 Å; C(δ)–C-8 distance 3.8 Å; C(δ)–C-1′ distance 3.8 Å; C(δ)–C-2′ distance 4.4 Å; ligand atoms are named as shown in Figure 10).

To validate the escitalopram-bound models obtained after MD simulations, we compared the ligand-binding site to the SSRI pharmacophore model to see if it agreed with the structural elements proposed by pharmacophore modeling. According to the SSRI-based hSERT pharmacophore,[8] two substrate features are important for recognition by hSERT: Feature 1: A basic

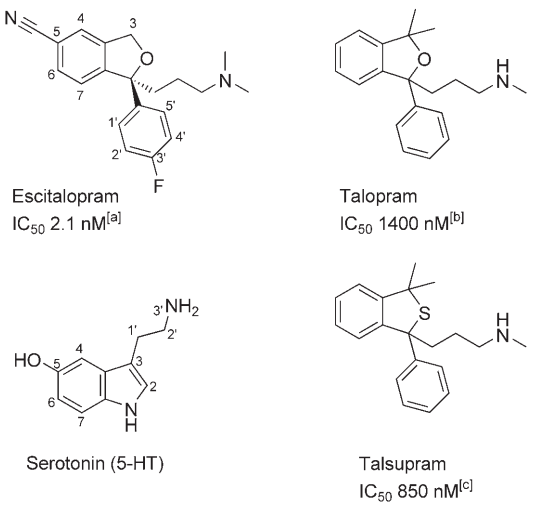

Figure 10. Chemical structures of compounds and IC_{50} values for 5-HT uptake inhibition. [a] Data from Ref. [6]; [b] data from Ref. [88]; [c] data from Ref. [89].

nitrogen having its lone pair pointing towards an acidic residue in the protein. The exact position of the nitrogen is less important. Feature 2: Two aromatic rings. In the SSRIs, only the aromatic centroids overlap in space. Additionally, the pharmacophore allows for substitution in the region corresponding to the cyano group in escitalopram (required for avoiding NET/DAT affinity),[8] and prohibits substituents in the region occupied by the hydrogens on C3 in escitalopram.

In our model, the salt bridge between D98 and the ligand explains the importance of Feature 1. Mutational studies have also revealed that such an ionic interaction is essential for escitalopram binding; the inhibitor displays very low affinity towards a D98E mutant.[53] With respect to Feature 2, the multiple hydrophobic interactions and in particular the π-π stackings established between the protein and the ligand aromatic rings contribute to the stability of the protein–ligand complex. The weak contact between fluorine and Y175 observed in the initial structure was not maintained during the simulation. Instead of mediating a direct protein–ligand contact, the fluorine may play a major role in the electron distribution in parts of the ligand. The same property can be expected for the cyano group and the oxygen atom. If opposite polarities dominate in the surrounding protein, such effects contribute significantly to the electrostatic interactions. In fact, an escitalopram analogue lacking two of the electron-withdrawing substituents, cyano and fluorine, displays 16-fold reduced affinity to hSERT compared to citalopram.[70] Visual inspection of the model structure indicates that the space available near the phthalane methylene group is sparse. Substituents other than hydrogens, such as in talopram and talsupram (see Figure 10 showing chemical structures), would sterically clash with the protein as predicted from our model. This observation suggests that the constructed hSERT models are in good agreement with the pharmacophore model.[8] Further ongoing studies using results from site-directed mutagenesis and variations in compound properties may provide additional insight into the determinants that govern ligand recognition.

Conclusions

We have carried out molecular dynamics simulations of hSERT in complex with 5-HT or escitalopram to study the binding modes of these ligands. We tested our membrane system by carrying out MD simulations on the *Aquifex aeolicus* leucine transporter. Atomic fluctuations extracted from the simulation were in good agreement with rmsd derived from the crystallographic B factor, thereby demonstrating that the system is suitable for gaining insight into the dynamic behavior of a membrane-embedded protein. During MD simulations of the hSERT complexes, we observed that the transporter relaxed into a conformation that can accommodate either 5-HT or escitalopram. The protein–ligand interactions in both protein–ligand complexes were in agreement with predictions from mutational studies and pharmacophore modeling. The substrate 5-HT establishes few key interactions to the protein, whereas a large number of strong and weaker interactions link the uptake inhibitor to the active site. Both ligands form a combined hydrogen bond/salt bridge to D98 via their protonated amines and interact through hydrophobic interactions with I172. In addition, the indole ring in 5-HT forms hydrogen bonds with G442 and T439, whereas escitalopram is in direct contact with Y176, F335, and F341 through π-π interactions. We observed that residue Y176 adopts different conformations, resulting in different protein–protein contacts in the hSERT–5-HT and hSERT–escitalopram complexes. When 5-HT is bound to the protein, Y176 forms a hydrogen bond with the D98 side chain, whereas in the hSERT–escitalopram complex, residue Y176 is in contact with S438. These differences in protein–protein contacts between the substrate- and inhibitor-bound states indicate that the ligands bind to hSERT by an induced fit mechanism[64,65] as observed, for instance, for ligand binding to P-glycoproteins and transferase.[66,67] Further studies using other NSS transporters are being pursued, and those results may provide further insights into structure–function relationships.

Computational Methods

Homology modeling and ligand docking

The escitalopram-optimized hSERT homology model was constructed as described by Jørgensen et al.[48] The terminal regions and the second extracellular loop regions are much longer in the mammalian than in the bacterial transporters, so for these three regions no structural template was available. Our primary focus was on the ligand-binding site to which these regions are located distally, and therefore these regions were left out of the model. Serotonin in its presumed bioactive conformation[9,71] was docked manually into the ligand-binding site in that model. Several binding modes were considered, but only one fulfilled the following four criteria: 1) D98-amine salt bridge,[9,53] 2) a hydrogen bond between the 5-HT hydroxyl group and the protein in which the hydroxyl group functions as hydrogen donor,[9] 3) protein to indole nitrogen proton polar interaction,[9] and 4) protein to indole skeleton hydrophobic interactions.[9] The binding site was subsequently energy-

minimized with the MMFF94 force field[72] available in MOE (using default parameters).[73]

Simulation system

Employing VMD,[74] the A*quifex aeolicus* leucine transporter including ligand, two sodium ions, a chloride ion, and crystal water[18], was solvated in a cubic simulation box with water. Applying in-house/noncommercial algorithms, water molecules occupying the putative membrane regions were replaced with three kinds of pseudo-carbon atoms: in water molecules located in the putative membrane core region (26 Å), the oxygen was replaced by an uncharged pseudo-carbon atom; in water molecules located in the putative head group regions (4 Å on each side), the oxygen was replaced by either positively (0.01 e) or negatively charged pseudo-carbon atoms (−0.01 e). Subsequently, all hydrogens belonging to these molecules were deleted. Each of the two regions containing charged atoms were organized into four 1 Å thick layers, alternately holding atoms with opposite charges. Negatively charged layers faced the membrane core region. The dimensions and charge organization of the membrane region resemble 1-palmitoyl-2-oleoyl-phosphatidylcholine (POPC) that is the major component of human neuronal plasma membranes.[75] All membrane-atoms were constrained in space by a weak harmonic potential (force constant $k = 0.02$ kcal mol^{-1} Å^{-2}). Two water layers with a thickness of about 15 Å remained at the top and bottom of the system. Chloride ions were subsequently added to compensate for the net positive charge of the system and to ensure an overall neutral system. The simulation box for LeuT consisted of 508 amino acid residues, 10199 water molecules, 3352 uncharged membrane atoms, 499 positively charged membrane atoms, 478 negatively charged membrane atoms, the leucine ligand, 2 sodium ions, and 7 chloride counter-ions. Altogether, there were a total of 43117 atoms in the system. The dimensions of the central unit cell were approximately $101 \times 81 \times 89$ Å^3. For hSERT, the simulation box had approximate dimensions of $113 \times 83 \times 97$ Å^3. It contained 49046 or 49066 atoms in total, comprised 507 amino acid residues, 12198 water molecules, 4452 uncharged membrane atoms, 499 positively charged membrane atoms, 478 negatively charged membrane atoms, the 5-HT or escitalopram ligand (26 or 46 atoms, respectively), 2 sodium ions, and 10 chloride counter-ions.

Molecular dynamics simulations

MD simulations were carried out using the NAMD2 package[76] with the CHARMM27 parameter set[77,78] and the TIP3 water model.[79] Full periodic boundary conditions were applied, and the simulations were carried out at constant number of atoms, constant pressure in the *z*-direction, constant area in the *x*-*y* plane, and constant temperature (NP_zAT ensemble). The Langevin piston method[80] with a damping coefficient of 6 ps^{-1} and a piston period of 100 fs imposed a constant ambient pressure of $P_z = 1$ atm. The temperature was held at 310 K. A time step of 1 fs was used in all simulations. Long-range Coulumb interactions were calculated using the Ewald summation technique[81,82] and updated every fourth step. For van der Waals interactions, a cut-off of 12 Å was applied in combination with a switching function starting at 10 Å.

At first, the simulation system was energy-minimized using the conjugate gradient method. In the initial LeuT simulation system, the particle density in the membrane region was too high, which resulted in a relatively high pressure in the *x*-direction ($p_y \sim 1$ atm). The minimization of this system was followed by short MD simulations, where the simulation box was consecutively expanded along the *x* axis to reach a pressure of $p_x \sim 1$ atm. Finally, this equilibrated system was submitted to 10 ns MD simulations.

Parameters for the ligands 5-HT and especially escitalopram were not available in the CHARMM27 force field,[77,78,83] requiring implementation of additional atom types and determination of force field parameters. Atomic charges for both ligands were obtained from the ESP charges estimated by ab initio single point energy calculations using Hartree Fock approximation with the 6-31G* basis set. Calculations were performed in Spartan.[84] Parameters for fluorine[85,86] and the cyano-group[87] were taken from the literature. Parameters for the cyclic ether group and for other undefined distances, angles, and torsions were obtained from CHARMM27 parameter set describing similar atom types, or in a few cases estimated empirically. Additionally, improper torsion constraints ($k = 10$ kcal mol^{-1} rad^{-2}) on heavy atoms in the 5-HT amino-ethyl side chain and in the escitalopram dimethylaminopropyl side chain ensured that the bioactive conformations of these ligands were maintained.

5-HT- or escitalopram-bound hSERT was introduced in the equilibrated model-membrane system by superimposing hSERT on LeuT. LeuT, leucine, ions, and water molecules located more than 8.5 Å from the binding site in the crystal structure were subsequently deleted. The remaining crystal waters were found to be important for maintaining the hydrogen-bonding networks in the protein interior in LeuT and hSERT. The escitalopram hSERT membrane systems were energy-minimized, followed by 100 ps simulations during which all atoms of the protein, ligand, NA1, and NA2, as well as crystal water were maintained in space by a harmonic potential with $k =$ 5 kcal mol^{-1} Å^{-2}. This should allow the water molecules and the atoms in the membrane layers to relax and pack around the protein. During an additional 100 ps simulation, harmonic distance constraints ($k = 100$ kcal mol^{-1} Å^{-2}) on the residue pairs D437(Oδ)–S438(Hγ), escitalopram(N)–D98(Oδ), and Y176(HH)–S438(Oγ) were used in order for the protein to adapt to the ligand. The entire system was subsequently subjected to 7 ns MD simulations without constraints. For 5-HT-bound hSERT, the first 100 ps of simulation time also included constraints on all protein and ligand atoms, sodium ions, and crystal water atoms. This was followed by 17 ns MD simulations without constraints.

Supporting information available

Sequence alignment (hSERT versus LeuT) and figures showing the overall fluctuations in the three protein complexes over

time, the time evolution of residue distances in LeuT, and figures showing the time evolution of distances between selected residues and NA1 and NA2 in LeuT, 5-HT-, or escitalopram-bound hSERT.

Acknowledgements

The authors gratefully acknowledge access to the Danish Center for Scientific Computing at the University of Southern Denmark. G.H. Peters acknowledges financial support from the Danish National Research Foundation via a grant to MEMPHYS-Center for Biomembrane Physics. A.M. Jørgensen acknowledges H. Lundbeck A/S and the Ministry for Science, Technology, and Innovation for an industrial PhD scholarship. Images were drawn with VMD[74] or MOE.[73]

Keywords: escitalopram · induced fit · molecular dynamics · molecular recognition · neurotransmitter transporters

[1] N. Nelson, *J. Neurochem.* **1998**, *71*, 1785 – 1803.
[2] G. Rudnick, J. Clark, *Biochim. Biophys. Acta Bioenerg.* **1993**, *1144*, 249 – 263.
[3] S. G. Amara, *Nature* **1992**, *360*, 420 – 421.
[4] S. G. Amara, M. J. Kuhar, *Annu. Rev. Neurosci.* **1993**, *16*, 73 – 93.
[5] G. R. Uhl, P. S. Johnson, *J. Exp. Biol.* **1994**, *196*, 229 – 236.
[6] J. Hyttel, *Int. Clin. Psychopharmacol.* **1994**, *9*, 19 – 26.
[7] C. Sanchez, P. B. Bergqvist, L. T. Brennum, S. Gupta, S. Hogg, A. Larsen, O. Wiborg, *Psychopharmacology* **2003**, *167*, 353 – 362.
[8] K. Gundertofte, K. P. Bøgesø, T. Liljefors in *Computer-Assisted Lead Finding and Optimization* (Eds.: H. v. d. Waterbeemd, B. Testa, G. Folkers), Wiley-VCH, Weinheim, **1997**, pp. 443 – 459.
[9] J. Pratuangdejkul, B. Schneider, P. Jaudon, V. Rosilio, E. Baudoin, S. Loric, M. Conti, J. M. Launay, P. Manivet, *Curr. Med. Chem.* **2005**, *12*, 2389 – 2406.
[10] S. G. Dahl, I. Sylte, A. W. Ravna, *J. Pharmacol. Exp. Ther.* **2004**, *309*, 853 – 860.
[11] A. W. Ravna, I. Sylte, S. G. Dahl, *J. Comput.-Aided Mol. Des.* **2003**, *17*, 367 – 382.
[12] A. W. Ravna, I. Sylte, S. G. Dahl, *J. Pharmacol. Exp. Ther.* **2003**, *307*, 34 – 41.
[13] A. W. Ravna, O. Edvardsen, *J. Mol. Graphics Modell.* **2001**, *20*, 133 – 144.
[14] A. W. Ravna, I. Sylte, K. Kristiansen, S. G. Dahl, *Bioorg. Med. Chem.* **2006**, *14*, 666 – 675.
[15] J. Abramson, S. Iwata, H. R. Kaback, *Mol. Membr. Biol.* **2004**, *21*, 227 – 236.
[16] J. Abramson, I. Smirnova, V. Kasho, G. Verner, H. R. Kaback, S. Iwata, *Science* **2003**, *301*, 610 – 615.
[17] Y. Huang, M. J. Lemieux, J. Song, M. Auer, D. N. Wang, *Science* **2003**, *301*, 616 – 620.
[18] A. Yamashita, S. K. Singh, T. Kawate, Y. Jin, E. Gouaux, *Nature* **2005**, *437*, 215 – 223.
[19] K. A. Williams, *Nature* **2000**, *403*, 112 – 115.
[20] C. Hunte, E. Screpanti, M. Venturi, A. Rimon, E. Padan, H. Michel, *Nature* **2005**, *435*, 1197 – 1202.
[21] N. R. Goldberg, T. Beuming, H. Weinstein, J. A. Javitch in *Strategies in Molecular Neuropharmacology* (Eds.: A. Schousboe, H. Bräuner-Osborne), Humana Press, Totowa, **2003**, pp. 213 – 234.
[22] L. Norregaard, U. Gether, *Curr. Opin. Drug Discov. Devel.* **2001**, *4*, 591 – 601.
[23] L. K. Henry, L. J. DeFelice, R. D. Blakely, *Neuron* **2006**, *49*, 791 – 796.
[24] T. Beuming, L. Shi, J. A. Javitch, H. Weinstein, *Mol. Pharmacol.* **2006**, *70*, 1630 – 1642.
[25] A. W. Ravna, M. Jaronczyk, I. Sylte, *Bioorg. Med. Chem. Lett.* **2006**, *16*, 5594 – 5597.
[26] C. M. Deber, N. K. Goto, *Nat. Struct. Biol.* **1996**, *3*, 815 – 818.
[27] W. F. van Gunsteren, F. J. Luque, D. Timms, A. E. Torda, *Annu. Rev. Biophys. Biomol. Struct.* **1994**, *23*, 847 – 863.
[28] M. Gross, *Curr. Protein Pept. Sci.* **2000**, *1*, 339 – 347.
[29] S. H. White, W. C. Wimley, *Annu. Rev. Biophys. Biomol. Struct.* **1999**, *28*, 319 – 365.
[30] J. Ballesteros, H. Weinstein, *Methods Neurosci.* **1995**, *25*, 366 – 428.
[31] T. M. Frimurer, R. P. Bywater, *Proteins Struct. Funct. Genet.* **1999**, *35*, 375 – 386.
[32] R. G. Efremov, D. E. Nolde, A. G. Konshina, N. P. Syrtcev, A. S. Arseniev, *Curr. Med. Chem.* **2004**, *11*, 2421 – 2442.
[33] M. C. Gershengorn, R. Osman, *Endocrinology* **2001**, *142*, 2 – 10.
[34] Y. Zhang, Y. Y. Sham, R. Rajamani, J. Gao, P. S. Portoghese, *ChemBioChem* **2005**, *6*, 853 – 859.
[35] A. A. Ivanov, I. I. Baskin, V. A. Palyulin, L. Piccagli, P. G. Baraldi, N. S. Zefirov, *J. Med. Chem.* **2005**, *48*, 6813 – 6820.
[36] A. Poulsen, B. Bjørnholm, K. Gundertofte, I. Pogozheva, T. Liljefors, *J. Comput.-Aided Mol. Des.* **2003**, *17*, 765 – 783.
[37] F. U. Axe, S. D. Bembenek, S. Szalma, *J. Mol. Graphics Modell.* **2006**, *24*, 456 – 464.
[38] D. P. Tieleman, H. J. Berendsen, M. S. P. Sansom, *Biophys. J.* **1999**, *76*, 1757 – 1769.
[39] D. P. Tieleman, H. J. Berendsen, *Biophys. J.* **1998**, *74*, 2786 – 2801.
[40] M. Bachar, O. M. Becker, *Biophys. J.* **2000**, *78*, 1359 – 1375.
[41] C. E. Capener, I. H. Shrivastava, K. M. Ranatunga, L. R. Forrest, G. R. Smith, M. S. Sansom, *Biophys. J.* **2000**, *78*, 2929 – 2942.
[42] Y. Xu, F. J. Barrantes, X. Luo, K. Chen, J. Shen, H. Jiang, *J. Am. Chem. Soc.* **2005**, *127*, 1291 – 1299.
[43] C. E. Capener, M. S. P. Sansom, *J. Phys. Chem. B* **2002**, *106*, 4543 – 4551.
[44] M. S. Sansom, P. J. Bond, S. S. Deol, A. Grottesi, S. Haider, Z. A. Sands, *Biochem. Soc. Trans.* **2005**, *33*, 916 – 920.
[45] D. P. Tieleman, H. J. C. Berendsen, M. S. P. Sansom, *Biophys. J.* **2001**, *80*, 331 – 346.
[46] S. G. Dahl, O. Edvardsen, I. Sylte, *Proc. Natl. Acad. Sci. USA* **1991**, *88*, 8111 – 8115.
[47] G. H. Peters in *Enzyme functionality: Design, Engineering, and Screening*, (Ed.: A. Svendsen), Marcel Dekker, New York, **2004**, pp. 97 – 148.
[48] A. M. Jørgensen, L. Tagmose, A. M. M. Jørgensen, S. Topiol, M. Sabio, K. Gundertofte, K. P. Bøgesø, G. H. Peters, *ChemMedChem* **2007**, *2*, 815 – 826.
[49] N.-H. Chen, M. E. A. Reith, in *Contemporary Neuroscience: Neurotransmitter Transporters: Structure, Function, and Regulation* (Ed.: M. E. A. Reith), Humana Press, Totowa, **2002**, pp. 53 – 109.
[50] J. Dunbrack, *Curr. Opin. Struct. Biol.* **2002**, *12*, 431 – 440.
[51] J. G. Chen, A. Sachpatzidis, G. Rudnick, *J. Biol. Chem.* **1997**, *272*, 28321 – 28327.
[52] J. G. Chen, G. Rudnick, *Proc. Natl. Acad. Sci. USA* **2000**, *97*, 1044 – 1049.
[53] E. L. Barker, K. R. Moore, F. Rakhshan, R. D. Blakely, *J. Neurosci.* **1999**, *19*, 4705 – 4717.
[54] M. B. Larsen, B. Elfving, O. Wiborg, *J. Biol. Chem.* **2004**, *279*, 42147 – 42156.
[55] H. M. Berman, J. Westbrook, Z. Feng, G. Gilliland, T. N. Bhat, H. Weissig, I. N. Shindyalov, P. E. Bourne, *Nucleic Acids Res* **2000**, *28*, 235 – 242.
[56] M. Bansal, S. Kumar, R. Velavan, *J. Biomol. Struct. Dyn.* **2000**, *18*, 811 – 819.
[57] E. Gouaux, *Curr. Opin. Struct. Biol.* **1997**, *7*, 566 – 573.
[58] G. Kieseritzky, G. Morra, E. W. Knapp, *J. Biol. Inorg. Chem.* **2006**, *11*, 26 – 40.
[59] G. Kamdar, K. M. Penado, G. Rudnick, M. M. Stephan, *J. Biol. Chem.* **2001**, *276*, 4038 – 4045.
[60] K. M. Penado, G. Rudnick, M. M. Stephan, *J. Biol. Chem.* **1998**, *273*, 28098 – 28106.
[61] L. K. Henry, E. M. Adkins, Q. Han, R. D. Blakely, *J. Biol. Chem.* **2003**, *278*, 37052 – 37063.
[62] G. A. Jeffrey, W. Saenger, *Hydrogen bonding in biological structures*, Springer, Berlin, **1994**.
[63] L. K. Henry, J. R. Field, E. M. Adkins, M. L. Parnas, R. A. Vaughan, M.-F. Zou, A. H. Newmann, R. D. Blakely, *J. Biol. Chem.* **2006**, *281*, 2012 – 2023.
[64] D. E. Koshland, Jr., *Proc. Natl. Acad. Sci. USA* **1958**, *44*, 98 – 104.
[65] J. A. McCammon, *Curr. Opin. Struct. Biol.* **1998**, *8*, 245 – 249.
[66] S. Eschenburg, M. A. Priestman, F. A. bdul-Latif, C. Delachaume, F. Fassy, E. Schonbrunn, *J. Biol. Chem.* **2005**, *280*, 14070 – 14075.

[67] T. W. Loo, M. C. Bartlett, D. M. Clarke, *J. Biol. Chem.* **2003**, *278*, 13603 – 13606.
[68] M. O. Sinnokrot, E. F. Valeev, C. D. Sherrill, *J. Am. Chem. Soc.* **2002**, *124*, 10887 – 10893.
[69] M. O. Sinnokrot, C. D. Sherrill, *J. Phys. Chem. A* **2004**, *108*, 10200 – 10207.
[70] K. P. Bøgesø, B. Bang-Andersen, in *Textbook of Drug Design and Discovery* (Eds.: P. Krogsgaard-Larsen, T. Liljefors, U. Madsen), Taylor & Francis, London, **2002**, pp. 299 – 327.
[71] L. B. Kier, *J. Pharm. Sci.* **1968**, *57*, 1188 – 1191.
[72] T. A. Halgren, *J. Comput. Chem.* **1996**, *17*, 490 – 519.
[73] Molecular Operating Environment, version 2005.06 Chemical Computing Group Inc., Montreal.
[74] W. Humphrey, A. Dalke, K. Schulten, *J. Mol. Graph.* **1996**, *14*, 33 – 38.
[75] D. A. White in *Form and Function of Phospholipids* (Eds.: G. D. Ansell, J. N. Hawthorne, R. M. C. Dawson), Elsevier Scientific Publishing, Amsterdam, **1973**, pp. 441 – 482.
[76] L. Kalé, R. Skeel, M. Bhandarkar, R. Brunner, A. Gursoy, N. Krawetz, J. Phillips, A. Shinozaki, K. Varadarajan, K. Schulten, *J. Chem. Phys.* **1998**, *151*, 283 – 312.
[77] B. D. Olafson, D. J. States, S. Svaminathan, M. Karplus, *J. Comput. Chem.* **1983**, *4*, 187 – 217.
[78] S. E. Feller, J. MacKerell, *J. Phys. Chem. B* **2000**, *104*, 7510 – 7515.
[79] W. L. Jorgensen, J. Chandrasekhar, J. D. Medura, R. W. Impey, M. L. Klein, *J. Chem. Phys.* **1983**, *79*, 926 – 935.
[80] S. E. Feller, Y. H. Zhang, R. W. Pastor, B. R. Brooks, *J. Chem. Phys.* **1995**, *103*, 4613 – 4621.
[81] T. Darden, D. York, L. Pedersen, *J. Chem. Phys.* **1993**, *98*, 10089 – 10092.
[82] U. Essmann, L. Perera, M. L. Berkowitch, T. Darden, L. P. L. G. Hsing, *J. Chem. Phys.* **1995**, *103*, 8593.
[83] A. D. MacKerell, D. Bashford, M. Bellott, R. L. Dunbrack, J. D. Evanseck, M. J. Field, S. Fischer, J. Gao, H. Guo, S. Ha, D. Joseph-McCarthy, L. Kuchnir, K. Kuczera, F. T. K. Lau, C. Mattos, S. Michnick, T. Ngo, D. T. Nguyen, B. Prodhom, W. E. Reiher, B. Roux, M. Schlenkrich, J. C. Smith, R. Stote, J. Straub, M. Watanabe, J. Wiorkiewicz-Kuczera, D. Yin, M. Karplus, *J. Phys. Chem. B* **1998**, *102*, 3586 – 3616.
[84] Spartan version '04 Wavefunction Inc., Irvine.
[85] "Parameterization for emperical force field calculations and a theoretical study of membrane permeability of pyrimidine derivative": D. Yin, PhD thesis, University of Maryland, **1997**.
[86] I. J. Chen, D. Yin, A. D. MacKerell, Jr., *J. Comput. Chem.* **2002**, *23*, 199 – 213.
[87] D. L. Luisi, C. D. Snow, J. J. Lin, Z. S. Hendsch, B. Tidor, D. P. Raleigh, *Biochemistry* **2003**, *42*, 7050 – 7060.
[88] J. McConathy, M. J. Owens, C. D. Kilts, E. J. Malveaux, V. M. Camp, J. R. Votaw, C. B. Nemeroff, M. M. Goodman, *Nucl. Med. Biol.* **2004**, *31*, 705 – 718.
[89] M. Schou, J. Sovago, V. W. Pike, B. Gulyas, K. P. Bøgesø, L. Farde, C. Halldin, *Mol. Imaging Biol.* **2006**, *8*, 1 – 8.

Received: October 18, 2006
Revised: March 6, 2007
Published online on April 13, 2007

